Microbial Ecology

Combining *in Situ* Reverse Transcriptase Polymerase Chain Reaction, Optical Microscopy, and X-ray Photoelectron Spectroscopy to Investigate Mineral Surface-Associated Microbial Activities

T.S. Magnuson, A.L. Neal and G.G. Geesey

Department of Microbiology and Center for Biofilm Engineering, Montana State University, Bozeman, MT 59717, USA

Received: 20 November 2003 / Accepted: 26 April 2004 / Online publication: 9 November 2004

Abstract

A study was undertaken to investigate expression of a gene encoding a *c*-type cytochrome in cells of the dissimilatory metal reducing bacterium (DMRB) *Geobacter sulfurreducens* during association with poorly crystalline and crystalline solid-phase Fe(III)-oxides. The gene encoding OmcC (outer membrane *c*-type cytochrome) was used as a target for PCR-based molecular detection and visualization of *omcC* gene expression by individual cells and aggregates of cells of *G. sulfurreducens* associated with ferrihydrite and hematite mineral particles. Expression of *omcC* was demonstrated in individual bacterial cells associated with these Fe-oxide surfaces by *in situ* RT-PCR (IS-RT PCR) and epifluorescence microscopy. Epifluorescence microscopy also permitted visualization of total DAPI-stained cells in the same field of view to assess the fraction of the cell population expressing *omcC*. By combining reflected differential interference contrast (DIC) microscopy and epifluorescence microscopy, it was possible to determine the spatial relationship between cells expressing *omcC* and the mineral surface. Introduction of the fluorescently labeled lectin concanavalin A revealed extracellular polymeric substances (EPS) extending between aggregations of bacterial cells and the mineral surface. The results indicate that EPS mediates an association between cells of *G. sulfurreducens* and ferrihydrite particles, but that direct cell contact with the mineral surface is not required for expression of *omcC*. XPS analysis revealed forms of reduced Fe associated with areas of the mineral surface where EPS-mediated bacterial associations occurred. The results demonstrate that by combining molecular biology, reflectance microscopy, and XPS, chemical transformations at a mineral surface can be related to the expression of specific genes by individual bacterial cells and cell aggregates associated with the mineral surface. The approach should be useful in establishing involvement of specific gene products in a wide variety of surface chemical processes.

Introduction

Dissimilatory metal reduction is an important environmental process in which microorganisms respire on high-valence metals and metal complexes. This process is being increasingly understood in terms of the physiology and biochemistry involved in the transformations of minerals [29, 30, 32, 35] and the chemical reactions that are associated with respiratory metal reduction [8, 9, 22, 25, 27, 28]. Iron-and manganese-reducing organisms of the genera *Geobacter* and *Shewanella* have served as convenient model organisms for a variety of reasons; many representative isolates are available in pure culture, the organisms are relatively easy to culture on a variety of iron compounds, and the biochemistry and genetics of these organisms are well characterized. While there are several noteworthy examples of research describing attachment to and growth of Fe-reducing bacteria on solid-phase iron oxides, and the iron transformations that result from these activities [3, 5–9], little is known about the genes that are expressed by the bacteria under these conditions. Childers et al. [5] showed expression of a gene in *Geobacte metallireducens* that putitatively encodes pili used for attachment of cells of to Fe(III) oxides.

Present address of T.S. Magnuson: Department of Biological Sciences, Idaho State University, Pocatello, ID 83204, USA
Present address of A.L. Neal: Department of Microbiology and Savannah River Ecology Laboratory, University of Georgia, Athens, GA 30602, USA
Correspondence to: G.G. Geesey; E-mail: gill_g@erc.montana.edu

 DOI: 10.1007/s00248-004-0253-x • Volume 48, 578–588 (2004)

The genome of *Geobacter sulfurreducens* has been sequenced, and several genes encoding cytochromes identified. Leang et al. [24] identified two genes *omcB* and *omcC* in *G. sulfurreducens* sharing 79% sequence homology that are expressed when cells are grown with either fumarate or Fe(III) citrate as the electron acceptor. Based on unreported results that an OmcC-deficient mutant grew as well as the wild type on soluble Fe(III) or poorly crystalline Fe(III), but that growth of an OmcB-deficient mutant was not sustainable with Fe(III) oxide as the electron acceptor, these authors suggested that OmcB is an important component in electron transport to Fe(III) but that OmcC is probably not. Thus, a role for OmcC remains to be established in this bacterium.

In this study we demonstrate the application of *in situ* reverse transcriptase–polymerase chain reaction (IS-RT PCR) and epifluorescence microscopy to detect expression of *omcC* in individual cells and cell aggregates of *G. sulfurreducens* associated with ferrihydrite and hematite surfaces when these solid-phase Fe(III) oxides serve as the sole electron acceptor in the system. X-ray photoelectron spectroscopy (XPS) revealed the presence of Fe(II) on the surface of the Fe(III) oxide in areas containing *omcC*-expressing cells. Such an approach offers new opportunities to relate expression of specific genes by mineral surface-associated cells to chemical transformations at the mineral surface at high spatial resolution.

Materials and Methods

Organism and Culture Conditions. *Geobacter sulfurreducens* strain PCA (ATCC 51573) [4] was grown on modified freshwater medium containing the following components (g/L): NH_4Cl (1.5); NaH_2PO_4 (0.6); KCl (0.1); $NaHCO_3$ (2.5); sodium acetate (0.82); Wolfe's Vitamin Solution (10.0 mL); modified Wolfe's minerals (10.0 mL). All cultures were grown at 30°C in anaerobic culture tubes under a 20% CO_2/80% N_2 atmosphere, and all culture manipulations were performed anaerobically. Acetate (20 mM), was provided as electron donor, and either soluble Fe(III) citrate (50 mM), synthetic hydrous ferric oxide (ferrihydrite) (10% w/v), or specular tabular hematite (0.5–2.0 mm particle size; 2 g/10 mL culture volume) from Bahia, Brazil [Stanford Mineralogical collection (#51080) provided by Dr. K. Rosso, Pacific Northwest National Laboratory, Richland, WA] provided as a sole electron acceptors.

Preparation and Analysis of DNA and RNA. Nucleic acids were prepared from 1-week-old cultures of *G. sulfurreducens* using commercial kits (Qiagen, Valencia, CA). Prior to RNA extraction, cultures were first treated with an RNase inhibitor. Nucleic acids were quantified by UV spectrophotometry. Integrity of RNA preparations was determined by formaldehyde gel electrophoresis [2].

PCR and RT PCR: omcC Amplification. Sequence information used to design primers for *G. sulfurreducens omcC* was obtained from the most recent release of the genome data for this bacterium (www.tigr.org). The primers, specific for *omcC*, amplify ~700 bp of the gene at its 5′ end. The primers used were 296F (5′-ACARMARSGRTGTYGGSTGC-3′) and 992R (5′-TGGATYMCSRGARGTYGYAGTG-3′). Careful design was performed to ensure that these primers recognized sequences only found in *omcC*, and not in the closely related gene *omcB*. PCR was carried out under the following conditions: 200 nM forward and reverse primer; 20 mM Tris-HCl pH 8.8; 50 mM KCl; 2.0 mM $MgCl_2$; 1.0 U *Taq* DNA polymerase (Promega Corp., Madison, WI); 0.1% Tween 20; and ~500 ng template DNA. Thermocycling began with a "hot-start" step of 5 min at 94°C followed by 30 cycles of 94°C for 30 s, 45°C for 1 min, and 72°C for 2 min and ended with a 7-min 72°C final extension. Primer specificity was confirmed as follows: PCR products were analyzed by agarose gel (1.7%) electrophoresis, and visualized with ultraviolet light after ethidium bromide staining. Individual fragments with the predicted size were purified from gel slices with a QIAquick Gel Extraction kit (Qiagen), according to the manufacturer's instructions. Products were cloned and plasmids extracted as above, and sequenced as described below using M13 forward and reverse primers.

RT PCR reactions contained 200 ng template RNA, 1 U of AMV-reverse transcriptase (Promega, Madison, WI), 1 U of Tfl-DNA polymerase (Promega), 50 mM Tris-HCl, 63 mM KCl, 10 mM $(NH_4)_2SO_4$, 5 mM dithiothrietol, and 10% (v/v) glycerol, 2 mM $MgSO_4$, 0.2 mM dNTP, 200 μM each of forward and reverse primers, in a total reaction volume of 20 μL. Reverse transcription was carried out at 48°C for 1 h, and after a 5-min RT inactivation step, PCR was continued using the reaction conditions described above. Products were analyzed as described above. Reactions carried out in the absence of reverse transcriptase were included as a control. It was not possible to include a negative control in which cells were growing in the absence of *omcC* expression, since no conditions have yet been identified under which wild-type cells can be cultivated without *omcC* expression [24].

In Situ RT PCR (IS-RT PCR). Five-day-old cultures of *Geobacter sulfurreducens* in which solid-phase ferrihydrite or hematite served as the sole electron acceptor were used for IS-RT PCR. The solid mineral phase and associated cells were recovered by centrifugation, immediately fixed with 4% paraformaldehyde, washed three times with PBS, and treated with lysozyme (0.1 mg/mL) for 15 min to permeabilize the cells. The solid mineral phase and associated cells were washed again three times with PBS and then treated with DNase (5 U/μL cell suspension) to digest DNA within the cells. The

DNase was inactivated by heat, the solid mineral phase and associated cells washed, and resuspended in deionized water. This solid mineral phase-associated cell preparation was then used as template for *in situ* RT-PCR (IS-RT PCR) experiments. Primers OMC296F and OMC992R (specific for *omcC*) were used, and RT-PCR was carried out using AMV reverse transcriptase and Tfl DNA polymerase in a reaction mix that was optimized for *in situ* experiments. Reactions contained 5 μL cell suspension, 1 U of AMV-reverse transcriptase (Promega Madison, WI), 1 U of Tfl-DNA polymerase (Promega), 50 mM Tris-HCl, 63 mM KCl, 10 mM $(NH_4)_2SO_4$, 5 mM dithiothrietol, 10% (v/v) glycerol, 2 mM $MgSO_4$, 0.2 mM dNTP, 0.05 mM BODIPY-14-dUTP (Molecular Probes, Eugene, OR), and 200 nM each of forward and reverse primers, in a total reaction volume of 20 μL. Reactions were carried out on a suspension of the solid mineral phase and associated cells in PCR tubes, with the same conditions listed above. Control reactions contained no reverse transcriptase. After RT PCR, the solid mineral phase and associated cells were washed three times with water and then stained with a solution of 4′,6-diamidino-2-phenylindole dihydrochloride (DAPI, Sigma Chemical Co., St. Louis, MO) in water for 10 min, followed by a brief destaining with deionized water to permit microscopic visualization of cells independent of gene expression. The particles and associated cells were then transferred to glass slides for microscopic observation.

Lectin-Binding Assay. ConcanavalinA-AlexaFluor 488 (ConA) lectin conjugate (Molecular Probes) was used to evaluate exopolysaccharide produced by suspended individual cells and particle-associated cells of *G. sulfurreducens* using a method adapted from Strathmann et al. [44]. Cells and cell/mineral suspensions were pelleted at 3000g for 10 min, and resuspended in 500 μL 50 mM phosphate with 50 mM NaCl pH 7.2 (PBS). Lectin conjugate was added to a final concentration of 5.0 μg/mL. DAPI was added simultaneously to achieve a final concentration of 2.0 μg/mL, and staining was carried out for 1 h. Suspensions of minerals particles and associated bacteria were washed with 1 mL PBS, and resuspended in 100 μL PBS. Microscopic examination was performed immediately following staining as described below.

Microscopy and Image Analysis. Microscopic examination of mineral particle surfaces and associated bacterial cells was performed using a Nikon Eclipse E800 microscope equipped with 40× and 60× objectives, DIC polarizing filters, and reflectance optics. For epifluorescence microscopy, samples were illuminated with a 100 W Hg-vapor discharge lamp, and fluorescent images obtained using the following filter cubes: UV-2A (DAPI), HYQ Cy5 (Cy5) or HYQ Cy3 (ConA-AlexaFluor 488). Image capture was performed using a Micromax RTE/CCD-732-7 (Princeton Instruments, Trenton, NJ) camera and MetaVue 5.0 software.

X-ray Photoelectron Spectroscopy. X-ray photoelectron spectroscopy (XPS) was employed to determine the valence state of Fe on uncolonized and colonized ferrihydrite and hematite particle surfaces, and the extent to which each Fe(III) oxide surface is covered by Fe(II) reduction product. XPS is a surface sensitive (sampling depth $\sim$ 100 Å) spectroscopic technique suited to the identification of chemical transformations at surfaces at relatively high spatial resolution. Spectra were collected on a Perkin-Elmer Physical Electronics Division Model 5600ci spectrometer (Perkin Elmer, Eden Prairie, MN). The spectrometer was calibrated employing the Au4$f_{7/2}$, Cu2$p_{3/2}$, and Ag3$d_{5/2}$ photopeaks with binding energies of 83.99, 932.66, and 368.27 eV, respectively. A consistent 400-μm spot size was analyzed on all surfaces using a monochromatized AlK_α ($h\nu$ = 1486.6 eV) X-ray source at 300 W and a pass energy of 46.95 eV for survey scans, and 11.75 eV for high-resolution scans. The system was operated at a base pressure of 10^{-8}–$10^{-9}\tau$. A consistent emission angle (2ϕ) of 45° was used throughout. Following baseline subtraction [42], curves were fit employing an 80% Gaussian: 20% Lorentzian line shape. A common problem associated with the analysis of insulating materials such as hematite is the accumulation of surface charge during spectral collection leading to photopeak shifts. This potential problem was overcome by the use of a 5 eV flood gun and by referencing of the principal Cl*s* photopeak (nominally due to carbon of the type $[\text{-}CH_2\text{-}CH_2\text{-}]_n$) to a binding energy ($E_b$) of 284.8 eV [46]. Hematite samples were wicked dry with paper tissue and mounted without any further preparation, while ferrihydrite samples were dried onto a Si wafer before mounting. All samples were mounted in preparation for XPS in an anaerobic glove box and transported to the spectrometer in a plate chamber sealed under an anaerobic atmosphere. Brief (<5 s) exposure to air was unavoidable during introduction of the samples into an N_2 flushed antechamber. This antechamber was then evacuated and the sample placed into the spectrometer itself.

Analysis of Fe Valence State. In the transition metals, unpaired electrons give rise to so-called multiplet states. These states may have widely differing E_b and may thus be represented in photoelectron spectra by different photopeaks. Any model capable of differentiating between Fe(III) and Fe(II) ions must take into account these multiplet states. Theoretical core *p* level models describing multiplet splitting associated with ferrous and ferric ions have been demonstrated by Gupta and Sen [15] and empirical proofs of these models substantiated by Pratt et al. [38]. Accordingly, here we fit ferric ion contributions to high-resolution Fe2$p_{3/2}$ core regions

with five peaks that decrease in intensity at increased E_b, all peaks having the same line shape. Ferrous ion contributions are represented by a major peak accompanied by a pair of multiplet peaks 0.9 eV either side of the major peak and a shake-up satellite at elevated E_b ($\Delta E_b \sim$ 6 eV) [31]. The relative intensities of the Fe(II) peaks are consistent with the aforementioned models and have been applied elsewhere to good effect in the identification of reduced iron in the presence of microorganisms [18, 34].

Aqueous Phase Fe(II) Determinations. Fe(II) was monitored in ferrihydrite- and hematite-containing cultures using the Ferrozine assay with ferrous ammonium sulfate as a standard [43]. The contribution of reduced Fe in the inoculum to Fe(II) in Fe(III)-oxide-containing cultures was evaluated by comparing the level of Fe(II) in ferrihydrite- and hematite-containing cultures receiving an inoculum of viable cells with cultures receiving a formalin-killed cell inoculum with equal amounts of reduced Fe. Formalin was also added to sterile culture medium containing ferrihydrite or hematite to assess the effect of formalin on the stability of these mineral phases. At various times after culture inoculation, 0.1-mL subsamples of culture medium containing only formalin, formalin-killed cells, or viable cells were retrieved with a syringe and the Fe(II) levels assayed immediately. In the case of hematite-containing cultures, only the hematite particle-free fraction was collected during culture incubation since particles were too large to retrieve by syringe. Only at the end of the incubation was Fe(II) associated with the particles assayed following treatment with 0.5 N HCl. Ferrihydrite-containing cultures were mixed to suspend the particles prior to sampling both solid and liquid phases by syringe. The samples were treated with 0.5 N HCl prior to determination of Fe(II).

Results

Aggregation of Cells of G. sulfurreducens and Ferrihydrite Particles. Ferrihydrite particles added as sole electron acceptor in a culture medium inoculated with cells of *G. sulfurreducens* accumulated an increasing number of bacterial cells over a 1-week incubation period when subsamples were recovered from cultures at daily intervals, stained with DAPI, and examined by epifluorescence microscopy (Fig. 1A). During this period, visual examination of the cultures revealed an increase in particle clumping (Fig. 1B). Both the number and size of the aggregates increased during culture incubation. Ferrihydrite particles incubated in sterile culture medium or in culture medium inoculated with a formalin-killed inoculum showed no evidence of clumping and, when exposed to DAPI, displayed no detectable fluorescence which could be mistaken for bacterial cells (data not shown).

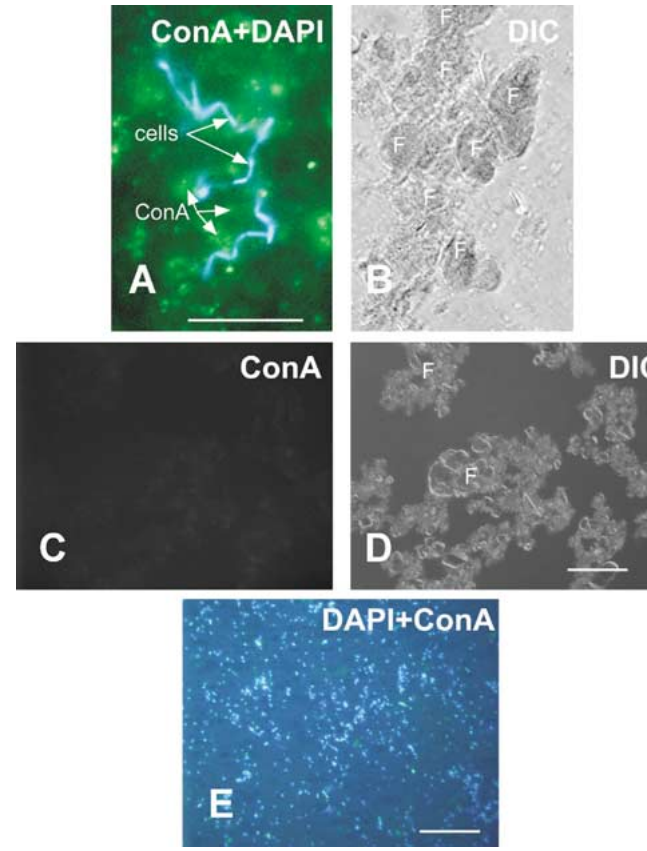

Figure 1. ConA-binding of extracellular material produced by cells of *G. sulfurreducens* recovered from 5-day cultures using ferrihydrite as sole electron acceptor. (A.) Epifluorescence microscopic image of DAPI-stained, ferrihydrite-associated cells (blue) surrounded by ConA-binding material (green). Bar = 10 μm. (B) Reflected DIC microscopic image of same field of view as A, showing location of aggregated ferrihydrite particles (F). (C) Epifluorescence microscopic image of ferrihydrite particles from sterile culture medium that have been exposed to fluorescently labeled ConA. Note absence of fluorescence in areas containing bacteria-free particles (F) revealed by reflected DIC microscopy in image D, which displays the same field of view as C (F). Bar = 10 μm. (E) Epifluorescence microscopic image of DAPI-stained, ConA-reacted, from a 5-day culture grown in medium containing soluble Fe(III) citrate as sole electron acceptor. Bar = 10 μm.

Fluorescently labeled ConA lectin, when added to 5-day cultures, reacted with extracellular polymeric substances (EPS) that extended between aggregated cells associated with ferrihydrite particles (Fig. 1A). The quantity of particle-associated ConA-reactive material increased during the time that the particle-associated bacterial numbers increased in the culture (data not shown). Ferrihydrite particles in uninoculated culture medium, when exposed to fluorescently labeled ConA, displayed no detectable fluorescence (Figs. 1C and 1D).

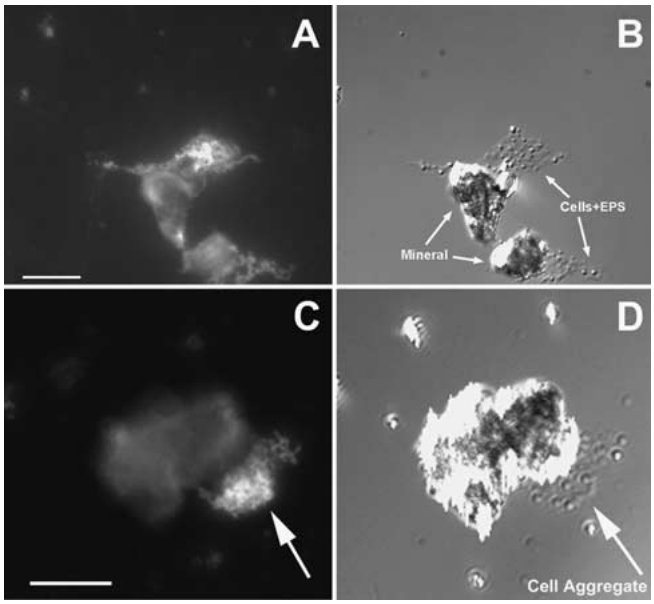

Figure 2. Ferrihydrite particles and associated cells of *G. sulfurreducens.* (A and C) Epifluorescence microscopic images showing location of fluorescently labeled *in situ* RT-PCR *omcC* gene products associated with ferrihydrite particles. (B and D) Reflected DIC microscopic images of the same fields of view as A and C, respectively, showing the location of ferrihydrite mineral particles and associated cells and extracellular material (EPS). Bar = 10 μm.

No ConA-reactive material was associated with cells recovered from 5-day cultures of *G. sulfurreducens* grown on soluble Fe(III) citrate (Fig. 1E). Evidence of an EPS matrix encapsulating aggregates of cells associated with the ferrihydrite particles was also obtained by reflected DIC microscopy (Fig. 2B). The EPS also appeared to extend between the encapsulated cells and the ferrihydrite mineral surfaces (Fig. 2B,D). Many of the EPS-encapsulated, particle-associated cells were not in direct contact with the ferrihydrite mineral surface.

Cells of *G. sulfurreducens* also attached to hematite particles when this crystalline Fe oxide was added to cultures as the sole electron acceptor. Epifluorescence microscopy of DAPI-stained particle preparations revealed primarily individual cells distributed randomly across the hematite surfaces recovered from 5-day cultures (Fig. 3B). Reflected DIC images of the same field of view revealed no obvious features on the mineral surface that influenced cell distribution (Fig. 3C). Occasionally, aggregations of cells resembling microcolonies were observed in some areas of the hematite surface (Fig. 4B).

RT PCR-Based Detection of omcC Expression by Cultures of G. sulfurreducens with Ferrihydrite as Sole Electron Acceptor. RT PCR analysis of mRNA extracted from 5-day cultures of *G. sulfurreducens* (ferrihydrite-associated + ferrihydrite-free cells) indicated that *omcC* was expressed under conditions in which ferrihydrite was the sole electron acceptor (Fig. 5). Control RT-PCR reactions carried out on mRNA samples from 5-day cultures in the absence of reverse transcriptase enzyme produced no detectable PCR product, indicating that the products generated in the presence of this enzyme were not derived from residual DNA remaining after DNase treatment (data not shown).

Gene Expression by Cells Associated with Mineral Surfaces. *omcC* gene expression was evaluated in intact cells associated with solid phase Fe(III) oxides using IS-RT PCR. Epifluorescence microscopy of ferrihydrite surface-associated cells from 5-day cultures, when subjected to IS-RT PCR using *omcC* specific primers and fluorogenic dNTPs, yielded brightly fluorescing areas (Fig. 2A,C) that correspond to areas occupied by aggregates of cells of *G. sulfurreducens* (Fig. 2B,D). Only faint background fluorescence was observed in areas of the ferrihydrite surface void of bacterial aggregates. Ferrihydrite particles recovered from uninoculated control cultures exhibited similar faint background fluorescence following subjection to the IS-RT PCR reaction, as did ferrihydrite particles recovered from inoculated cultures when reverse transcriptase enzyme was deleted from the IS-RT PCR reaction. Thus, EPS-encapsulated cells associated with, but not necessarily in direct contact with, ferrihydrite particle surfaces express *omcC* when ferrihy-

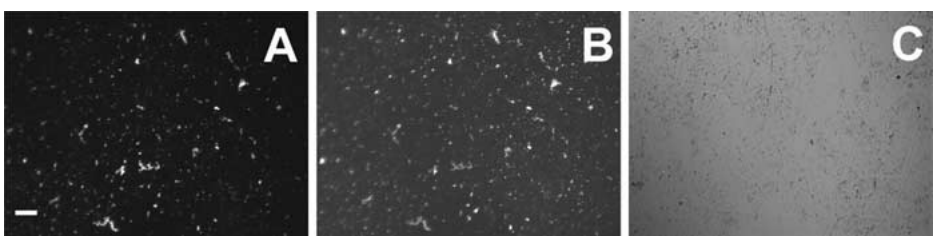

Figure 3. Surface of hematite particle following exposure to a 5-day culture of *G. sulfurreducens.* (A) Epifluorescence microscopic image showing location of fluorescently labeled *in situ* RT-PCR *omcC* gene products associated with particle surface. (B) Epifluorescence microscopic image of hematite surface showing location of DAPI-stained cells in the same field of view as A. (C) Reflected DIC microscopic image of hematite surface. Bar = 10 μm.

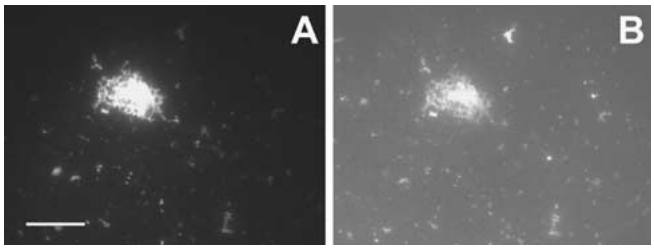

Figure 4. Aggregate of cells of *G. sulfurreducens* on hematite particle surface. Epifluorescence microscopic image showing (A) location of fluorescently labeled cDNA following IS-RT PCR using *omcC*-specific primers, and (B) location of DAPI-stained cells. Bar = 10 μm.

drite is supplied as the sole electron acceptor in the system.

Cells colonizing and forming aggregates on hematite particles also expressed *omcC*. When fluorescent images identifying the locations of IS-RT PCR products on hematite particle surfaces recovered from 5-day cultures of *G. sulfurreducens* (Fig. 3A) are superimposed on fluorescent images revealing the locations of DAPI-stained bacterial cells (Fig. 3B), the majority of hematite surface-associated, DAPI-stained cells, including those in microcolony-like aggregates (Fig. 4A,B) appeared to express the *omcC* gene.

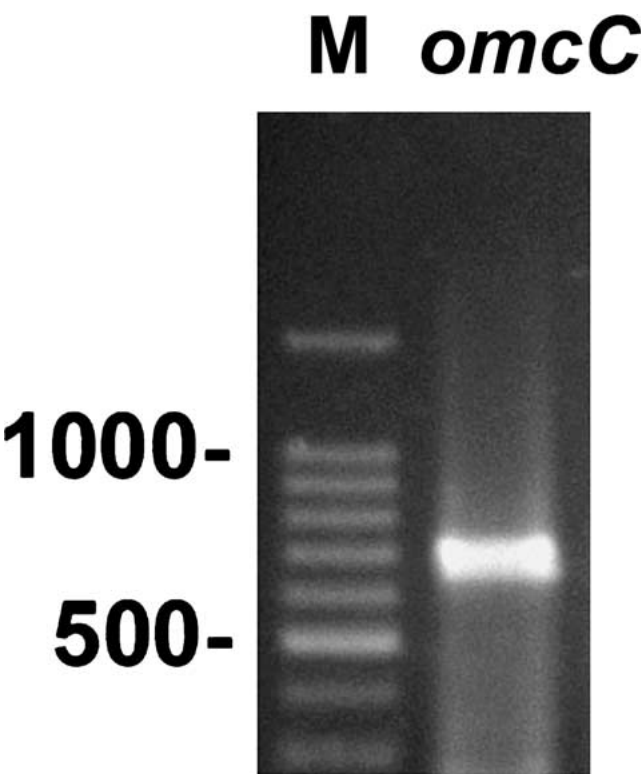

Figure 5. Agarose gel showing RT PCR product using as a template *omcC* mRNA-specific primers and total RNA from a culture of *G. sulfurreducens* grown on ferrihydrite. DNA ladder markers are in lanes M.

Spectroscopic Analysis of Bacteria-Free and Bacteria-Colonized Iron Oxide Mineral Surfaces. XPS of ferrihydrite and hematite particle surfaces prior to and following a 5-day exposure to sterile, anaerobic culture medium yielded spectra with a core Fe2$p_{3/2}$ peak envelope that adequately fit the Fe(III) multiplet splitting model and is in agreement with published iron oxide spectra [22, 31], suggesting that no abiotic Fe reduction occurred under these conditions (Table 1). In contrast, surfaces of ferrihydrite and hematite exposed for 5 days to a culture of *G. sulfurreducens* that used the same anaerobic medium as above yielded XP spectra for which the Fe(III) model no longer provided an adequate description of the observed core Fe2$p_{3/2}$ peak envelope. Addition of principal Fe(II) peaks at 708.1 and 708.4 eV for the hematite and ferrihydrite spectra, respectively (together with associated multiplet and satellite peaks), was required to complete the models. The extent to which Fe(II) accumulated on or remained associated with the mineral surface were markedly different for these two Fe(III) oxides. The extent to which Fe(II) covered the Fe(III) oxide mineral surface was estimated by comparing the area under the peaks contributed by Fe(II) to the total area under the core Fe2$p_{3/2}$ peak envelope [Fe(II) + Fe(III)]. Fe(II) contributed 53.3 at % of the total surface Fe on ferrihydrite particles, and 7.5 at % of the total surface Fe on hematite particles (Fig. 6).

The Fe(II) from the Fe(III) citrate–grown starter culture used to inoculate the hematite-containing media was unable to account for all the Fe(II) detected during cultivation of cells of *G. sulfurreducens* on media containing this solid-phase mineral. This was established by comparing the level of Fe(II) in the aqueous phase of a culture receiving an inoculum of viable cells to the level of Fe(II) in the aqueous phase of media inoculated with formalin-killed cells containing the same amount of Fe(II). Whereas the level of Fe(II) in the aqueous phase of cultures inoculated with viable cells increased during culture incubation, the level of Fe(II) in the aqueous phase of the culture receiving the formalin-killed cells decreased over time (Fig. 7A). Hematite exhibited no reactivity toward formalin in sterile culture medium over the same period of hematite exposure to the formalin-killed cell inoculum. The difference between Fe(II) levels in cultures receiving the viable and formalin-killed inocula represents the solution-phase Fe(II) derived from bacterial reduction of the Fe(III) oxides. At the end of the experiment, the solid phase of cultures receiving the viable cell inoculum contained 168 ± 10 nmol Fe(II)/g, whereas, the solid phase of cultures receiving a formalin-killed cell inoculum contained 72 ± 2 nmol Fe(II)/g (Fig. 7A). Thus, the portion of the mineral surface-associated Fe(II) detected by XPS derived from the Fe(II) pool produced through bioreduction of hematite was more than twice that attributable to that carried over in

Table 1. Binding energy data and interpretation of the results of curve fitting to Fe2$p_{3/2}$ core region spectra collected on uncolonized and colonized iron oxides

Sample	*E_b(eV)*[a]	*FWHM*[b]	*Area (at. %)*	*Chemical state*
Uncolonized hematite	709.4	1.4	39.8	Fe(III) multiplet 1
	710.3	1.4	32.2	Fe(III) multiplet 2
	711.5	1.4	16.5	Fe(III) multiplet 3
	712.4	1.4	7.2	Fe(III) multiplet 4
	713.4	1.4	5.1	Fe(III) multiplet 5
Uncolonized ferrihydrite	708.7	1.4	17.2	Fe(III) multiplet 1
	709.6	1.4	32.3	Fe(III) multiplet 2
	710.7	1.4	27.4	Fe(III) multiplet 3
	711.9	1.4	15.4	Fe(III) multiplet 4
	713.3	1.4	7.8	Fe(III) multiplet 5
Colonized hematite	708.1	1.6	3.8	Fe(II) multiplet 1
	707.2	1.3	2.0	Fe(II) multiplet 2
	709.0	1.3	1.2	Fe(II) multiplet 3
	714.1	2.3	0.5	Fe(II) satellite
	709.8	1.4	34.3	Fe(III) multiplet 1
	710.7	1.4	20.0	Fe(III) multiplet 2
	711.4	1.4	20.0	Fe(III) multiplet 3
	712.5	1.4	12.9	Fe(III) multiplet 4
	713.6	1.4	5.3	Fe(III) multiplet 5
Colonized ferrihydrite	708.4	1.6	27.2	Fe(II) multiplet 1
	707.5	1.3	14.4	Fe(II) multiplet 2
	709.3	1.3	8.2	Fe(II) multiplet 3
	713.8	2.3	3.5	Fe(II) satellite
	709.5	1.4	12.6	Fe(III) multiplet 1
	710.5	1.4	14.8	Fe(III) multiplet 2
	711.8	1.4	8.3	Fe(III) multiplet 3
	712.8	1.4	6.1	Fe(III) multiplet 4
	714.2	1.4	5.0	Fe(III) multiplet 5

[a]All E_b are referenced to a C1*s* photopeak of 284.8 eV.
[b]Full width at half maximum.

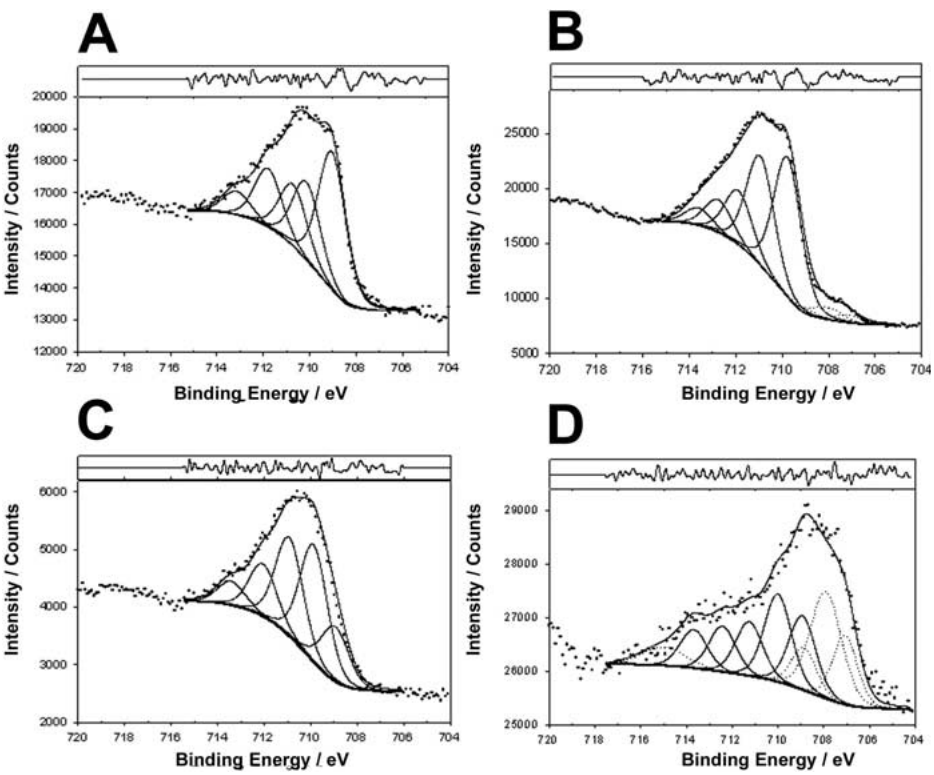

Figure 6. High resolution Fe2$p_{3/2}$ XPS spectra of hematite particle surface upon recovery from (A) uninoculated and (B) 5-day cultures of *G. sulfurreducens.* XPS spectra in C and D are from the surface of a ferrihydrite particle recovered from uninoculated and 5-day cultures of *G. sulfurreducens*, respectively. Peaks delineated by broken lines represent contribution of Fe(II). The area under these peaks relative to the total Fe2$p_{3/2}$ peak area reflects portion of the mineral surface analyzed that contains Fe(II).

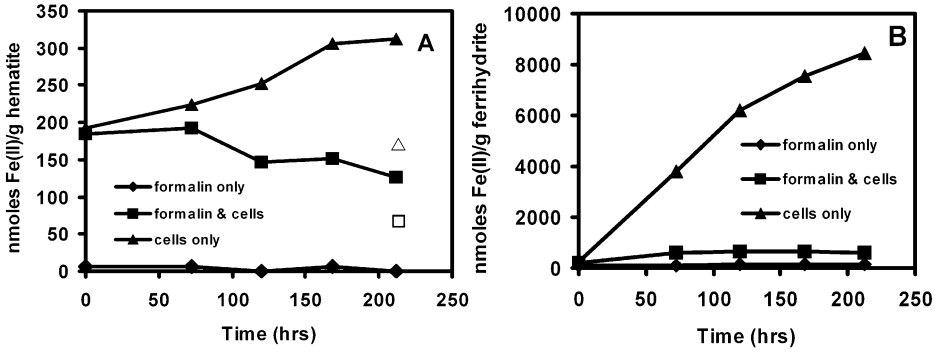

Figure 7. Fe(II) levels in cultures containing hematite (A) and ferrihydrite (B). Fe(II) levels were determined in particle-free aqueous phase fractions (solid symbols) of the hematite-containing cultures over the 212 h incubation period and in the solid-phase fraction (open symbols) at the end of the incubation period. Fe(II) levels in ferrihydrite-containing cultures were obtained from culture subsamples containing both solid and aqueous phases.

the culture inoculum. Together, the solid and aqueous phases of hematite-containing cultures receiving the viable cell inoculum contained 480 ± 36 nmol Fe(II)/g at the end of the 212-h incubation, whereas the combined solid and aqueous phases of cultures receiving a formalin-killed cell inoculum contained 198 ± 15 nmol Fe(II)/g. These results indicate that cells of *G. sulfurreducens* reduce hematite when added as sole electron acceptor in the culture. It is important to note, however, that the rate and extent of hematite reduction by cells of *G. sulfurreducens* are considerably less than for ferrihydrite. The maximum rate of hematite reduction without accounting for surface area differences was 1 nmol/h/g hematite particles compared to a maximum rate of 48 nmol/h/g ferrihydrite particles, while the extent of hematite reduction [282 nmol Fe(II)] was 4% of that [7813 nmol Fe(II)] obtained for ferrihydrite at the end of the 212-h experiment (Fig. 7A,B).

Discussion

IS-RT PCR Analysis of Cytochrome Expression during Cell Association with Fe(III) Oxide Surfaces. *In situ* RT PCR has been used previously to detect expression at the single cell level of genes involved in hydrocarbon degradation by *Pseudomonas* spp. and model marine bacterial communities [19], in universal stress response by archaea [23], and to detect expression of genes controlling physiological status in *Salmonella typhimurium* at the population level [20]. In this study we were able to adapt RT PCR to assess the expression of the c-type cytochrome-encoding gene *omcC* at the single cell level in cells aggregated at ferrihydrite and hematite surfaces. To our knowledge, this is the first report demonstrating the use of *in situ* RT PCR to monitor gene expression in individual cells of dissimilatory iron-reducing bacteria (DIRB) associated with solid-phase phase Fe(III) oxides. Our results clearly demonstrate that *omcC* is expressed by ferrihydrite- and hematite-associated cells of *G. sulfurreducens* when either of these Fe(III)-oxide phases serves as the sole electron acceptor. The results of the IS-RT PCR also reveal that cells associated with but not necessarily in direct contact with ferrihydrite particles express *omcC* and, thus appear to be active. Whether these cells produce an active gene product remains to be determined.

A role for OmcC has yet to be established. A recent study reported that both *omcB* and *omcC* are expressed by cells of *G. sulfurreducens* in logarithmic-phase cultures using either fumarate or Fe(III) citrate as the electron acceptor [24]. These investigators further suggested that because an *omcC* knockout mutant of *G. sulfurreducens* grows as well as the wild-type on Fe(III) citrate and poorly crystalline Fe(III) oxide, that OmcC is not likely to be an important component in electron transport to Fe(III) in this bacterium [24]. This evidence alone, however, does not preclude *omcC* from playing a role in respiratory reduction of solid-phase Fe(III) oxides by this DMRB. For example, while OmcC may not be required for Fe(III) oxide reduction under the conditions tested to date, it may still transfer electrons to Fe(III) under these conditions. It may also play a more essential role under conditions in which OmcB is not produced or active.

Mechanism of Mineral–Bacterial Cell Association. The detection and distribution of ConA-reactive material between cells of *G. sulfurreducens* associated with ferrihydrite particles suggests that cells synthesize and excrete extracellular polysaccharides containing terminal α-D-mannose and α-D-glucose residues [39]. Other DMRB have been shown to excrete extracellular polymers during growth on hematite and goethite [1]. Genes with sequences similar to those know to be involved in exopolysaccharide synthesis in other bacteria exist in the *G. sulfurreducens* genome (http://www.tigr.org). That cells associated with ferrihydrite were encapsulated by ConA-reactive material while cells recovered from cultures of

similar age containing soluble Fe(III) citrate in place of solid-phase Fe(III) as sole electron acceptor appeared free of this material suggests that this material may be produced and used by cells to establish close physical association with solid-phase electron acceptors.

The microscopic images revealed that many of the cells associated with ferrihydrite particles were not in direct contact with the particle surface, but tethered to the particle by EPS. Since *G. sulfurreducens* reportedly does not utilize small, soluble organic molecules as electron shuttles [45], it is unclear whether particle-associated cells encapsulated by EPS have access to the solid phase Fe(III) for respiration. Grantham et al. [14] suggested that a microbially induced local reduction in pH at an iron oxyhydroxide surface coating colonized by *Shewanella putrefaciens* promoted Fe(III) solubilization and surface pitting. The EPS of many bacteria contain acidic subunits (uronic acids), some of which have been shown to promote solubilization of solid phase metals [11–13, 21]. It remains to be determined whether the EPS of *G. sulfurreducens* contains acidic groups that solubilize Fe(III) and make it available to cells not in direct contact with the solid-phase Fe(III) oxide. Assessment of activity of bacterial cells at different locations within cell aggregates the size of those associated with ferrihydrite requires surface analytical methods with high spatial resolution.

The DMRB *Geobacter metallireducens* expresses flagella and pili to establish contact with insoluble Fe(III) and Mn(II) when used as the electron acceptor for cell growth [5]. While the genome of *G. sulfurreducens* also contains genes for the biosynthesis of Type IV pili (http://www.tigr.org), the expression of these genes and detection of pili in cells associated with insoluble electron acceptors has not yet been demonstrated. It is not uncommon for bacteria to synthesize pili to establish initial contact with solid surfaces and then synthesize and excrete extracellular polysaccharides during replication and microcolony development [16, 17, 36] Together, these studies suggest a suite of genes that could serve as suitable targets for IS-RT PCR analysis of events associated with DMRB attachment to, and colonization and reduction of Fe(III) oxide surfaces.

Evidence of Fe Reduction in Areas of a Mineral Particle Surface Containing DMRB. By combining XPS, IS-RT PCR, and reflectance microscopy, it was possible to detect Fe(II) product on the surfaces of aggregated ferrihydrite particles and on the surface of hematite particles within a 0.126 mm^2 area containing aggregations of *omcC*-expressing cells of *G. sulfurreducens*. Since Fe(II) carried over in the culture inoculum could not account for the majority of Fe(II) that accumulated over time in both the aqueous and solid phases of cultures containing hematite as the only other Fe source, the bulk of the mineral surface-associated Fe(II) appeared to be derived from the pool of Fe(II) produced from bioreduction of the hematite. While cultures of *G. sulfurreducens* have previously been shown to reduce, respire, and grow on amorphous solid-phase Fe oxides such as ferrihydrite [4], evidence of the ability of *Geobacter* spp. to reduce crystalline forms of Fe(III) oxides such as hematite has been difficult to obtain [26], possibly because of the limited reactivity of these phases and nature of the biochemical reactions involved in the reduction. The data presented here provide clear evidence that cells of *G. sulfurreducens* reduce crystalline-phase hematite, but at a rate and to an extent much less than observed for the poorly crystalline phase ferrihydrite. Other DMRB have also been shown to reduce hemitate at low rates [1, 26, 47]. The impact of low rates of bioreduction of crystalline phase Fe(III) oxides over geological time may be significant, although this has yet to be determined.

Whether reduction of hematite supports growth of *G. sulfurreducens* and other DMRD remains an open question Detecting small differences in viable cell biomass associated with particulate Fe is problematic [10]. A recently developed real-time, nondestructive microscopic approach used to quantify accumulation of cells of *Desulfovibrio desulfuricans* strain G20 and *Shewanella oneidensis* strain MR1 growing on specular hematite may prove useful in evaluating growth of *G. sulfurreducens* on this crystalline Fe(III) oxide [33, 34]. That cells expressed a *c*-type cytochrome gene when associated with hematite surfaces during periods of Fe(II) reduction indicates the cells are at least active under these conditions, and possibly engaged in Fe respiration.

It has been suggested that the observed decrease in rate of solid-phase Fe(III) oxide bioreduction after extended periods of reduction is the result of a decrease in Fe(III) surface area due to surface accumulation of reduction products [40, 41]. In contrast to the chemical extraction methods used to quantify reduction products associated with the solid phase [10, 40, 41], XPS offers the opportunity to quantify the extent to which the Fe(III) oxide surface is covered with reduction products. The results presented here indicate that $\sim$ 53% of the total Fe at the ferrihydrite surface and 7.5% of the total Fe at the hematite surface was converted to or overlaid with Fe(II) product after 5 days of exposure to cells of *G. sulfurreducens*. Thus, the decrease in rate of bioreduction of ferrihydrite observed here and by others after a period of active bioreduction was likely due, at least in part, to a reduction in Fe(III) surface area caused by the accumulation of Fe(II) reduction products. Fe(III) surface area alone did not appear to control the rate of Fe bioreduction on hematite, however, since Fe(III) still contributed >90% of the total surface Fe when reduction rates based on aqueous-phase Fe(II) decreased and eventually ceased. Rather, the rate of Fe(III) reduction

was likely controlled by surface structure in the case of crystalline hematite [33]. Crystalline-Fe(III) oxides are considered less reactive than amorphous Fe(III) oxide phases [37, 41, 47].

In summary, the results revealed that cells of *G. sulfurreducens* associated with poorly crystalline ferrihydrite particles produce lectin-reactive extracellular material, presumably polysaccharide in nature, which promotes formation of cell aggregates and retention of the aggregates at the particle surface. IS-RT PCR revealed that the majority of cells associated with these particles as well as particles of crystalline hematite express *omcC*, a gene encoding a *c*-type cytochrome. XPS revealed that cells of *G. sulfurreducens* reduce crystalline as well as amorphous Fe(III)-oxide phases and that some of the Fe(II) that is produced accumulates in areas of these oxide surfaces where *omcC*-expressing cells accumulate. IS-RT PCR provides a new approach to detect specific genes expressed by individual cells associated with environmentally relevant minerals and should aid in identification of the suite of genes expressed by cells associated with mineral surfaces during dissimilatory metal reduction.

Acknowledgments

Funding was provided by grant DE-FG-ER62994 (to T.S.M.) and DE-FG03-01ER63270 (to G.G.G.) from the Natural and Accelerated Bioremediation Research Program, Office of Biological and Environmental Research, U.S. Department of Energy, by grant MCB0132022 (to G.G.G) from the National Science Foundation, Microbial Observatory Program, and by a grant (to A.L.N) from the Office of Naval Research, Program Element 060223371.

References

1. Arnold, RG, DiChristina, TJ, Hoffman, MR (1988) Reductive dissolution of Fe(III) oxides by *Pseudomonas* sp. 200. Biotechnol Bioeng 32: 1081–1096
2. Ausabel, FM, Brent, R, Kingston, RE, Moore, DD, Seidman, JG, Smith, JA, Struh, K (1997) Current Protocols in Molecular Biology. John Wiley and Sons, New York
3. Caccavo Jr, F (1999) Protein-mediated adhesion of the dissimilatory Fe(III)-reducing bacterium BrY to hydrous ferric oxide. Appl Environ Microbiol 65: 5017–5022
4. Caccavo Jr, F, Lonergan, DJ, Lovley, DR, Davis, M, Stolz, J, McInerney, MJ (1994) *Geobacter sulfurreducens* sp. nov., a hydrogen- and acetate-oxidizing dissimilatory metal-reducing microorganism. Appl Environ Microbiol 60: 3752–3759
5. Childers, SE, Ciufo, S, Lovley, DR (2002) *Geobacter metallireducens* accesses insoluble Fe(III) oxide by chemotaxis. Nature 416: 767–769
6. Das, A, Caccavo Jr, F (2001) Adhesion of the dissimilatory Fe(III)-reducing bacterium *Shewanella alga* BrY to crystalline Fe(III) oxides. Curr Microbiol 42: 151–154
7. Das, A, Caccavo Jr, F (2000) Dissimilatory Fe(III) oxide reduction by *Shewanella alga* BrY requires adhesion. Curr Microbiol 40: 344–347
8. Dong, H, Fredrickson, JK, Kennedy, DW, Zachara, JM, Kukkadapu, RK, Onstott, TC (2000) Mineral transformation associated with the microbial reduction of magnetite. Chem Geol 169: 299–318
9. Fredrickson, JK, Zachara, JM, Kennedy, D, Duff, MC, Gorby, YA (2000) Reduction of U(VI) in goethite (α-FeOOH) suspensions by a dissimilatory metal-reducing bacterium. Geochim Cosmochim Acta 64: 3085–3098
10. Fredrickson, JK, Zachara, JM, Kennedy, DW, Dong, H, Onstott, TC, Hinman, NW, Li, S (1998) Biogenic iron mineralization accompanying the dissimilatory reduction of hydrous ferric oxide by a groundwater bacterium. Geochim Cosmochim Acta 62: 3229–3257
11. Geesey, GG, Costerton, JW (1986) "The microphysiology of consortia within adherent bacterial populations." pp 238–242, In: *4th International Symposium on Microbial Ecology.* Ljubljana, Yugoslavia
12. Geesey, GG, Jang, L, Jolley, JG, Hankins, MR, Iwoaka, T, Griffiths, PR (1988) Binding of metal ions by extracellular polymers of biofilm bacteria. Wat Sci Technol 11/12: 161–165
13. Geesey, GG, Mittelman, MW, Iwoaka, T, Griffiths, PR (1986) Role of bacterial exopolymers in the deterioration of metallic copper surfaces. Mat Perform 25: 37–40
14. Grantham, MC, Dove, PM, DiChristina, TJ (1997) Microbially catalyzed dissolution of iron and aluminum oxyhydroxide mineral surface coatings. Geochim Cosmochim Acta 61: 4467–4477
15. Gupta, RP, Sen, SK (1975) Calculation of multiplet structure of core *p*-vacancy levels. II. Phys Rev B 12: 15–19
16. Harrison, OB, Robertson, BD, Faust, SN, Jepson, MA, Goldin, RD, Levin, M, Heyderman, RS (2002) Analysis of pathogen–host cell interactions in Purpura Fulminans: expression of capsule, Type IV pili, and PorA by *Neisseria meningitidis in vivo.* Infect Immun 70: 5193–5201
17. Head, NE, Yu, H (2004) Cross-sectional analysis of clinical and environmental isolates of *Pseudomonas aeruginosa*: biofilm formation, virulence, and genome diversity. Infect Immun 72: 133–144
18. Herbert, RB, Benner, SG, Pratt, AR, Blowes, DW (1998) Surface chemistry and morphology of poorly crystalline iron sulfides precipitated in media containing sulfate-reducing bacteria. Chem Geol 144: 87–97
19. Hodson, RE, Dustman, WA, Garg, RP, Moran, MA (1995) *In situ* PCR for visualization of microscale distribution of specific genes and gene products in procaryotic communities. Appl Environ Microbiol 61: 4074–4082
20. Holmstrom, K, Tolker-Neilsen, T, Molin, S (1999) Physiological states of individual *Salmonella typhimurium* cells monitored by in situ reverse transcription-PCR. J Bacteriol 181: 1733–1738
21. Jolley, JG, Geesey, GG, Hankins, MR, Wright, RB, Wichlacz, PL (1988) Auger electron spectroscopy and X-ray photoelectron spectroscopy of the biocorrosion of copper by gum arabic, BCS and *Pseudomonas atlantica* exopolymer. J Surf Interface Anal 11: 371–376
22. Junta-Rosso, JL, Hochella, MF (1996) The chemistry of hematite (001) surfaces. Geochim Cosmochim Acta 60: 305–314
23. Lange, M, Tolker-Nielsen, T, Molin, S, Ahring, BK (2000) *In situ* reverse transcription-PCR for monitoring gene expression in individual *Methanosarcina mazei* S-6 cells. Appl Environ Microbiol 66: 1796–1800
24. Leang, C, Coppi, MV, Lovley, DR (2003) OmcB, a c-type polyheme cytochrome, involved in Fe(III) reduction in *Geobacter sulfurreducens.* J Bacteriol 185: 2096–2103

25. Lloyd, JR, Sole, VA, Van Praagh, CV, Lovley, DR (2000) Direct and Fe(II)-mediated reduction of technetium by Fe(III)-reducing bacteria. Appl Environ Microbiol 66: 3743–3749
26. Lovley, DR, Phillips, EJ (1988) Novel mode of microbial energy metabolism: organic carbon oxidation coupled to dissimilatory reduction of iron and manganese. Appl Environ Microbiol 54: 3234–3236
27. Lovley, DR, Phillips, EJP (1994) Reduction of chromate by *Desulfovibrio vulgaris* (Hildenborough) and its c_3 cytochrome. Appl Environ Microbiol 60: 726–728
28. Lovley, DR, Widman, PK, Woodward, JC, Phillips, EJP (1993) Reduction of uranium by cytochrome c_3 of *Desulfovibrio vulgaris.* Appl Environ Microbiol 59: 3572–3576
29. Magnuson, TS, Hodges-Myerson, AL, Lovley, DR (2000) Characterization of a membrane-bound NADH-dependent Fe^{3+} reductase from the dissimilatory Fe^{3+}-reducing bacterium *Geobacter sulfurreducens.* FEMS Microbiol Lett 185: 205–211
30. Magnuson, TS, Isoyama, N, Hodges-Myerson, AL, Davidson, G, Maroney, MJ, Geesey, GG, Lovley, DR (2001) Isolation, characterization and gene sequence analysis of a membrane-associated 89 kDa Fe(III) reducing cytochrome c from *Geobacter sulfurreducens.* Biochem J 359: 147–152
31. McIntyre, NS, Zetaurk, DG (1977) X-ray photoelectron spectroscopic studies of iron oxides. Anal Chem 49: 1521–1529
32. Myers, JM, Myers, CR (2001) Role for outer membrane cytochromes OmcA and OmcB of *Shewanella putrefaciens* MR-1 in reduction of manganese dioxide. Appl Environ Microbiol 67: 260–269
33. Neal, AL, Rosso, KM, Geesey, GG, Gorby, YA, Little, BJ (2003) Surface structure effects on direct reduction of iron oxides by *Shewanella oneidensis.* Geochim Cosmochim Acta 67: 4489–4503
34. Neal, AL, Techkarnjanaruk, S, Dohnalkova, A, McCready, D, Peyton, BM, Geesey, GG (2001) Iron sulfides and sulfur species produced at hematite surfaces in the presence of sulfate-reducing bacteria. Geochim Cosmochim Acta 65: 223–235
35. Newman, DK, Kolter, R (2000) A role for excreted quinones in extracellular electron transfer. Nature 405: 94–97
36. Paranjpye, RN, Lara, JC, Pepe, JC, Pepe, CM, Strom, MS (1998) The Type IV leader Peptidase/N-methyltransferase of *Vibrio vulniflcus* controls factors required for adherence to HEp-2 cells and virulence in iron-overloaded mice. Infect Immun 66: 5659–5668
37. Postma, D (1993) The reactivity of iron oxides in sediments: a kinetic approach. Geochim Cosmochim Acta 57: 5027–5034
38. Pratt, AR, Muir, IJ, Nesbitt, HW (1994) X-ray photoelectron and Auger electron spectroscopic studies of pyrrhotite and mechanism of air oxidation. Geochim Cosmochim Acta 58: 827–841
39. Quintero, EJ, Weiner, RM (1995) Evidence for the adhesive function of exopolysaccharide of *Hyphomonas* strain MHS-3 in its attachment to surfaces. Appl Environ Microbiol 61: 1897–1903
40. Roden, EE, Urrutia, MM (1999) Ferrous iron removal promotes microbial reduction of crystalline iron(III) oxides. Environ Sci Technol 33: 1847–1853
41. Roden, EE, Zachara, JM (1996) Microbial reduction of crystalline iron(III) oxides: influence of oxide surface area and potential for cell growth. Environ Sci Technol 30: 1618–1628
42. Shirley, DA (1972) High-resolution X-ray photoemission spectrum of the valence bands of gold. Phys Rev B 5: 4709–4714
43. Stookey, LL (1970) Ferrozine: a new spectrophotometric reagent for iron. Anal Chem 42: 779–782
44. Strathmann, M, Wingender, J, Flemming, HC (2002) Application of fluorescently labelled lectins for the visualization and biochemical characterization of polysaccharides in biofilms of *Pseudomonas aeruginosa.* J Microbiol Methods 50: 237–248
45. Straub, KL, Schink, B (2003) Evaluation of electron-shuttling compounds in microbial ferric iron reduction. FEMS Microbiol Lett 220: 229–233
46. Swift, P (1982) Adventitious carbon — the panacea for energy referencing? Surf Interface Anal 4: 47–51
47. Zachara, JM, Fredrickson, JK, Li, S-M, Kennedy, DW, Smith, SC, Gassman, PL (1998) Bacterial reduction of crystalline Fe^{3+} oxides in single phase suspensions and subsurface materials. Am Mineral 83: 1426–1443